A One-Dimensional Model of a Carbon-Black Slurry-Fueled Combustor

S.R. Turns* and G.M. Faeth†
The Pennsylvania State University, University Park, Pennsylvania

Results of a one-dimensional model of a carbon-black slurry-fueled combustor are presented. The model incorporates a shrinking-sphere analysis developed earlier to treat combustion of the carbon-black agglomerates that form as a result of drying of slurry drops. The agglomerate combustion analysis uses a $C\text{-}O_2\text{-}CO_2\text{-}H_2O$ reaction mechanism along with empirical factors to represent effects of pores in the agglomerates on density, transport rates, and reaction surface area. The one-dimensional model was used to predict effects of initial agglomerate diameter, chamber pressure, secondary-air scheduling, reference velocity, the presence of catalyst, and carbon-black composition on combustor performance. The findings suggest that agglomerate combustion is largely diffusion-controlled under practical combustor conditions, minimizing effects of carbon-black composition and catalyst on combustor performance. Simplified scaling laws for percent carbon burnout are developed to assist interpretation of combustor performance measurements.

Nomenclature

a_i = area/reactivity factor
A = combustor cross-sectional area
C_D = drag coefficient
C_p = specific heat
D = mixture diffusivity
i = enthalpy
K = dimensionless burning rate, $\dot{m}_c'' r_p / (\rho_g D)$
Le = Lewis number
m = mass
$\dot{m}$ = mass flow rate
$\dot{m}'$ = mass flow rate per unit length
M_i = molecular weight of species i
Nu = Nusselt number
n = power-law exponent
P = pressure
Pr = Prandtl number
q_r' = radiant heat transfer per unit length
q_c'', q_r'' = convective and radiative heat flux
r = radius
R = gas constant
R_i = reaction rate of species i
Re = Reynolds number
t = time
T = temperature
V = velocity
x = axial coordinate
x_a = length over which secondary air is injected
y = atomic hydrogen to carbon ratio
ϵ = extent of reaction
ϵ' = emissivity
ζ = transport enhancement factor
η_c = combustion efficiency based on carbon burnout
ρ = density
σ = Stefan-Boltzmann constant
ϕ = equivalence ratio

Subscripts

a = air
c = carbon
g = gas or gas phase
h = hydrogen
OA = overall
p = particle
ref = reference
s = stoichiometric
w = wall
wb = wet bulb
0 = initial

Presented as Paper 84-0126 at the AIAA 22nd Aerospace Sciences Meeting, Reno, Nev., Jan. 9-12, 1984; received May 15, 1984; revision received Sept. 7, 1984.

*Assistant Professor, Department of Mechanical Engineering. Member AIAA.

†Professor, Department of Mechanical Engineering. Member AIAA.

Introduction

CARBON-black slurries are of interest due to their potential as high-energy-density liquid fuels for volume-limited air-breathing propulsion systems.[1] The objective of the present investigation is to develop a simplified model of combustor operation with these fuels in order to assist fuel and combustor development efforts.

Past work has shown that high-performance carbon-black slurry fuels can be formulated and burned.[2-5] It was found, however, that longer residence times than those required for conventional liquid fuels were required to obtain good combustion efficiency. In order to obtain a better understanding of this combustion efficiency problem, the combustion properties of individual carbon-black slurry drops were studied in previous investigations.[6-8] Results from these studies were used to develop the present combustor model.

The first of these earlier studies considered the combustion of individual carbon-black slurry drops supported at various points within a turbulent diffusion flame burning in air.[6] It was found that combustion was a two-stage process. The first stage involved heat-up and gasification (drying) of the liquid fuel, leaving all of the carbon-black particles originally in the drop as a porous solid agglomerate. The second stage involved continued heat-up and reaction of the agglomerate. The second stage was generally more than an order of magnitude longer than the first; therefore, agglomerate reaction is the rate-controlling step in carbon-black slurry combustion and its slowness is the main reason for the increased combustor residence time requirements for these fuels.

Efforts were also made to develop a model for the combustion lifetime (variation of diameter, liquid mass, carbon

mass, and temperature as a function of time) of carbon-black slurry drops.[6-8] The liquid gasification stage was relatively conventional and was successfully modeled using techniques developed for analysis of drops in sprays.[6] A new model of agglomerate reaction was developed taking the particle to be a shrinking sphere with empirical factors defined to treat effects of pores on particle density, convection transport rates, and reaction area.[6,7] Two carbon reaction mechanisms were considered with equivalent results: 1) the $C/O_2/OH$ mechanism of Neoh et al.[9] and 2) a $C/O_2/CO_2/H_2O$ mechanism which was an extension of an approach used by Libby and Blake.[10,11] The empirical parameters of the model were found to be relatively independent of initial agglomerate diameter (in the 10-1000-μm range) and flame conditions (fuel equivalence ratios of 0.2-1.4, flame temperatures of 800-1950 K at atmospheric pressure). However, the empirical parameters varied significantly with extent of agglomerate reaction and were influenced, to a lesser degree, by carbon-black composition and the presence of catalyst. Simple correlations were found to represent these variations of empirical parameters which yielded good predictions of combustion lifetimes for the wide range of conditions mentioned earlier.

The purpose of the present investigation was to extend these findings by applying the carbon-black slurry combustion model to a simplified analysis of a slurry-fueled combustor. The model was then used for a parametric investigation of combustion chamber characteristics which sought guidelines for combustor design and fuel formulation. Parameters considered included initial carbon agglomerate size, chamber pressure, secondary-air schedule, mass loading, initial agglomerate temperature, initial slip velocity, carbon-black composition, and catalyst loading.

Combustor Model

General Description

In the following, a carbon-black slurry combustor is modeled as a one-dimensional flow consisting of a dilute mixture of agglomerate particles and products of combustion. This implies that the volume occupied by agglomerate particles is negligible. With this approach, it was assumed that the relatively slow-burning carbon-black agglomerates survive the primary combustion zone (where all the liquid fuel is assumed to be burned) and subsequently burn out in the secondary zone. Mixing rates among the secondary air, the particle products of combustion, and the bulk gas are assumed to be infinitely fast throughout the secondary zone.

Initial gas-phase conditions, at the start of agglomerate combustion, are determined by assuming adiabatic combustion of the liquid fuel component (taken to be JP-10) without any combustion of solid carbon in the primary zone. Following recent practice with carbon-black slurry combustors,[3] the fuel equivalence ratio of the primary was taken to be unity, based on combustion of the liquid fuel alone. Air to complete combustion of the agglomerates and to dilute the combustion products was assumed to be added in the secondary zone, using schedules to be defined later. Agglomerate combustion rates were found using the agglomerate combustion model developed earlier.[6-8] The present analysis incorporates the extended Libby and Blake[10,11] mechanism along with the assumption of equilibrium reactant concentrations at the particle surface. Based on past experience,[6,8] use of the Neoh et al.[9] mechanism would yield similar results. The agglomerates were assumed to be monodisperse at the start of reaction, although the model can be readily extended to treat polydisperse size distributions. The initial agglomerate temperature was taken to be equal to the wet-bulb temperature for liquid evaporation, corresponding to the end of the first stage of slurry drop combustion,[6] although parametric variations from this level were also considered. Various levels of initial agglomerate slip were also considered. Typical of most one-dimensional combustor models, axial diffusion in the continuous phase was ignored.

Governing Equations

Mass Conservation

The rate of change of gas-phase mass flow rate with distance along the combustor is

$$\frac{d\dot{m}_g}{dx} = -\frac{d\dot{m}_c}{dx} + \dot{m}'_a \tag{1}$$

where $\dot{m}_a$ is the rate of secondary-air addition per unit length specified by the secondary-air schedule. The solid-phase carbon mass flow rate can be expressed in terms of the initial solid carbon mass flow rate and the extent of solid carbon reaction as follow:

$$\dot{m}_c = \dot{m}_{c0}(1-\epsilon) \tag{2}$$

For all agglomerate blends and flame conditions considered in earlier works,[7,8] agglomerate density can be represented reasonably well by

$$\rho_p = \rho_{p0}(1-\epsilon)^{0.6} \tag{3}$$

Expressing the particle mass in Eq. (2) in terms of the particle density and volume and substituting Eq. (3), yields the following expression for the local value of the agglomerate radius;

$$r_p = r_{p0}(1-\epsilon)^{0.13} \tag{4}$$

The rate of change of the extent of reaction was calculated using the agglomerate reaction model of Szekely and Faeth[6] and Szekely et al.[8] with boundary conditions found assuming thermodynamic equilibrium in the gas phase. The governing equation for ϵ is

$$-\frac{1}{\dot{m}_{c0}}\frac{d\dot{m}_c}{dx} = \frac{d\epsilon}{dx} = \left(\frac{4\pi r_p^2}{\dot{m}_{c0} V_p}\right)\sum_i a_i R_i \tag{5}$$

where i represents O_2, CO_2, and H_2O. In general, R_i depends on particle surface properties, the local gas environment, the relative velocity of the particle, and the empirical transport enhancement factor. The transport enhancement factor is a multiplicative function greater than unity applied to both the Sherwood and Nusselt numbers to account for the convective gas motion through the porous, and sometimes lacy, agglomerates. The area/reactivity factors, a_i, are also multiplicative functions but are applied to the chemical kinetic rates[10,11] to account for the increased surface area of the porous agglomerate in comparison to the smooth sphere used in the analysis. Both empirical parameters are functions of ϵ, r_{p0}, and the relative proportions of the different carbon blacks having different particles sizes which make up the agglomerate. The complete formulation for R_i and correlations for the empirical parameters are presented in Refs. 6-8.

The gas-phase mass balances are as follows:

$$\dot{m}_{cg} = \dot{m}_{cg0} + \epsilon\dot{m}_{c0} \tag{6a}$$

$$\dot{m}_a = \dot{m}_{a0} + \int_0^x \dot{m}'_a dx \tag{6b}$$

$$\dot{m}_h = \dot{m}_{h0} \tag{6c}$$

Equations (6) provide the mass flow rates of elements in the gas phase. Combining these results with information on the

gas-phase enthalpy (to be discussed next), the gas-phase composition was found assuming thermodynamic equilibrium and an ideal gas mixture. The analyses of Olikara and Borman[12,13] were used for the thermodynamic equilibrium calculations.

Under the same assumptions, neglecting the volume of the agglomerates as well, the local gas velocity was computed from the following:

$$V_g = (\dot{m}_{cg} + \dot{m}_a + \dot{m}_h) RT_g / (PA) \tag{7}$$

where R is the gas constant for the local gas mixture.

Energy Conservation

The overall energy balance of the combined solid and gas phases yields

$$\frac{\mathrm{d}(\dot{m}_g i_g)}{\mathrm{d}x} = -\frac{\mathrm{d}(\dot{m}_c i_c)}{\mathrm{d}x} + \dot{m}_a' i_a - q_r' \tag{8}$$

where the enthalpy of the secondary air i_a is specified as a boundary condition. The radiation heat loss was estimated, assuming optically thin conditions, by

$$q_r' = 4\pi \dot{m}_{c0} \epsilon' \sigma r_p^2 (T_p^4 - T_w^4) / (m_{p0} V_p) \tag{9}$$

where T_w is specified as a boundary condition. The enthalpy change of the solid phase can be expressed as

$$\frac{\mathrm{d}(\dot{m}_c i_c)}{\mathrm{d}x} = \dot{m}_c C_{pc} \frac{\mathrm{d}T_p}{\mathrm{d}x} + i_c \frac{\mathrm{d}\dot{m}_c}{\mathrm{d}x} \tag{10}$$

assuming that the particle temperature is uniform. Conservation of energy for a particle, under the same assumption, yields[6]

$$\frac{\mathrm{d}T_p}{\mathrm{d}x} = \left(\frac{-3}{\rho_p C_{pp} r_p V_p}\right)\left[\sum_i a_i R_i (i_p - i_c) + q_c'' + q_r''\right] \tag{11}$$

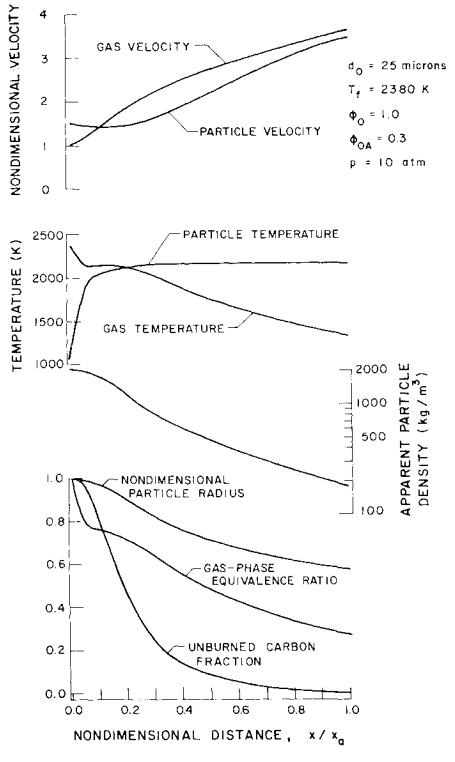

Fig. 1 Agglomerate particle-life history and combustor environment.

where

$$q_c'' = \frac{\lambda_g K (i_g - i_p)}{C_{pg} r_p [1 - \exp(2K/\zeta NuLe)]} \tag{12}$$

with the Nusselt number given by[14]

$$Nu = 2 + \frac{0.552\, Re^{1/2} Pr^{1/3}}{[1 + 1.232/(RePr^{4/3})]^{1/2}} \tag{13}$$

Momentum Conservation

The pressure gradient along the combustor was assumed to be negligible; therefore, the gas-phase momentum equation is trivial. Effects of body forces were neglected. Virtual mass and Basset forces were neglected since $\rho_p \gg \rho_g$, except near the end of the particle lifetime when the density of the lacy agglomerate becomes quite small, as given by Eq. (3). However, particle slip is also quite small. Conservation of particle momentum then becomes

$$\frac{\mathrm{d}V_p}{\mathrm{d}x} = -3C_D \rho_g (V_p - V_g) |V_p - V_g| / (8\rho_p r_p V_p) \tag{14}$$

In the absence of other information, the drag coefficient was taken to be the same as a smooth sphere, as follows[15]:

$$C_D = 24/Re + 6/(1 + Re^{1/2}) + 0.4 \tag{15}$$

To complete the model, the residence time of an agglomerate in the secondary region was obtained by integrating

$$\frac{\mathrm{d}t}{\mathrm{d}x} = V_p^{-1} \tag{16}$$

Solution

After substituting Eq. (10) into Eq. (8), a set of five coupled ordinary differential equations must be solved, e.g., Eqs. (5), (8), (11), (14), and (16). A detailed formulation is given in Ref. 16. These equations were integrated using a fourth-order Adams predictor-corrector method after specifying appropriate initial conditions at the start of the secondary zone. This solution provided local values of unburned carbon fraction, gas- and solid-phase temperatures, gas and particle velocities, and gas-phase composition.

Table 1 Variable combustor parameters[a]

Parameter	Level		
	Low	Standard	High
Agglomerate particle diameter, μm	10	25	50,75,100
Chamber pressure, atm	1	10	20
Nondimensional reference velocity[b]	0.5	1.0	2.0
Initial particle slip ratio, V_{p0}/V_{ref}	1.0	1.5	2.0
Initial particle preheat, $(T_{p0} - T_{wb})/(T_f - T_{wb})$	0	0.25	0.50
Catalyst addition	—	No	Yes
Ultimate particle size, nm	70	300	—

[a] The standard secondary air schedule consisted of a constant air injection rate per unit length up to a nondimensional length of 1.0. A ramp schedule was a linear distribution decreasing to zero at a nondimensional length of 1.0. The spike schedule was a constant air injection rate per unit length up to a nondimensional length of 0.10.

[b] Reference velocity as used herein is defined as the velocity of the gas emerging from the primary zone prior to addition of secondary air.

Parametric Investigation

Parameter Indentification

To provide guidelines for combustor design, the influence of carbon agglomerate diameter, chamber pressure, secondary-air schedule, and nondimensional reference were evaluated using the one-dimensional model. Effects of agglomerate slip velocity and degree of agglomerate preheat upon emergence from the primary zone were also evaluated, since these parameters appear in the model as unknown initial conditions. Three or more levels of these six parameters were chosen to be representative of the likely range of values in practical combustors. These parameters are shown in Table 1 with the central value used as the "standard" value. Calculations were carried out with all but one parameter fixed at the standard level, except as noted. The effects of catalyst addition and ultimate particle diameter were also investigated at two levels, based on their effect on the empirical parameters of the agglomerate combustion model.

Interaction of the above parameters with the primary zone parameters was ignored. Thus, for example, the effect of chamber pressure on the primary zone flame temperature was neglected to isolate the effects of pressure in the secondary zone. Values of fixed parameters are given in Table 2.

Results

Figure 1 illustrates the typical history of an agglomerate particle as it moves downstream through the changing combustor environment. The downstream distance has been normalized by the length over which secondary air is injected. This length was chosen so that 98% of the solid carbon was consumed by the end of air addition for the standard set of parameters. From the figure, it can be seen that the initial burning rate is quite low until the particle temperature reaches the range 1500-1700 K. This is followed by relatively rapid burning up to a dimensionless distance of roughly 0.25, after which the burning rate begins to decrease. Aside from the initial heat-up period, the particle temperature exceeds the gas temperature by several hundred degrees, suggesting the diffusion-control burning dominates the carbon burnout process. The gas-phase equivalence ratio is controlled principally by secondary-air addition until the carbon combustion rate accelerates (after a nondimensional distance of roughly 0.08). The gas velocity increases monotonically as additional mass enters the gas phase from both secondary-air injection and carbon combustion. With the specified initial slip velocity, the agglomerate particle slows down to zero slip at a dimensionless distance of approximately 0.10. Thereafter, the particle is accelerated by the gas phase, approaching zero slip again at the end of the lifetime, when the particle becomes small.

The influence of the first five combustor parameters given in Table 1 and secondary-air schedule on carbon burnout is shown in Figs. 2-7. In each of these figures, the unburned carbon fraction is plotted as a function of distance through the secondary zone. The termination of each curve represents approximately 98% complete carbon combustion.

As can be seen in Fig. 2, the effect of initial particle diameter is quite marked, with the length required for 98% combustion efficiency increasing more than an order of magnitude as initial particle size increases from 10 to 100 μm. This result is not unexpected since for diffusion-controlled combustion, individual particle burning rates, $d(d_p)/dt$, are roughly inversely proportional to particle diameter.[6,7] To quantify the influence of agglomerate diameter—as well as the other parameters investigated—exponents for a power-law-type dependence of burning time on parameter variation were calculated for various values of extent of reaction ϵ, i.e.,

$$(t_1/t_2)_{\epsilon=\text{constant}} = (\mathcal{P}_1/\mathcal{P}_2)^n \qquad (17)$$

Table 2 Fixed combustor paramters

Primary zone flame temperature, T_f	2380 K
Secondary-air temperature, T_a	700 K
Solid carbon weight loading	56%
Primary zone equivalence ratio, ϕ_0	1.0
Overall equivalence ratio, ϕ_{OA}	0.30
Ultimate particle diameter, d_u	300 nm
Nondimensional length of secondary-air injection zone	1.0

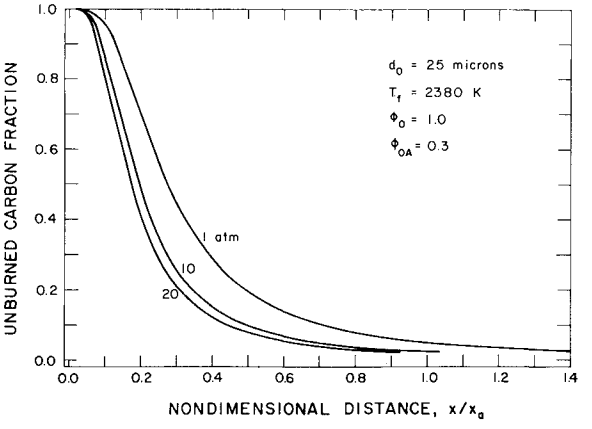

Fig. 3 Unburned carbon fraction vs nondimensional distance for chamber pressure of 1, 10, and 20 atm.

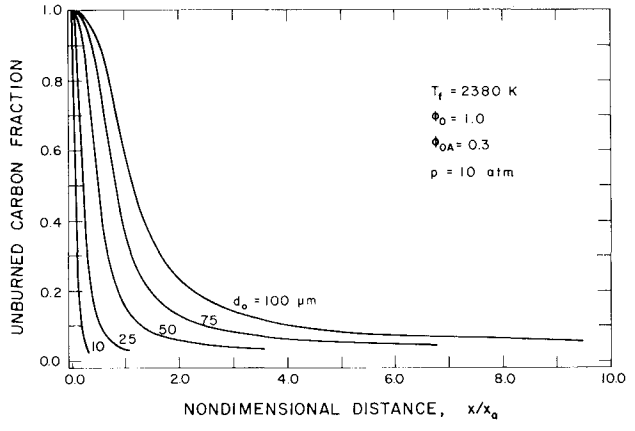

Fig. 2 Unburned carbon fraction vs nondimensional distance for initial agglomerate diameters ranging from 10 to 100 μm.

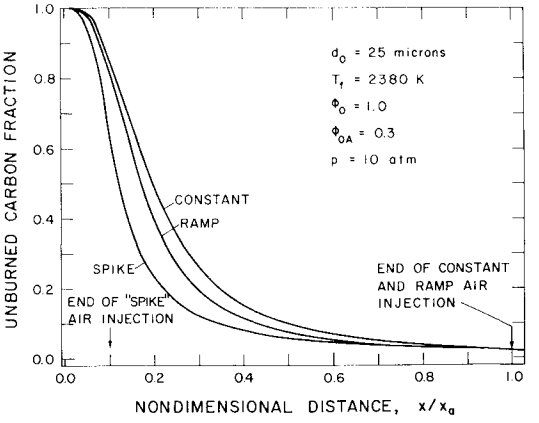

Fig. 4 Unburned carbon fraction vs nondimensional distance for three different secondary-air schedules.

Table 3 Burning time power-law exponents

Parameter	$\epsilon = 5\%$	$\epsilon = 50\%$	$\epsilon = 95\%$
Agglomerate particle diameter	1.32	1.26	1.39
Chamber pressure	-0.192	-0.153	-0.156
Reference velocity, fixed air injection length	-0.268	-0.324	-0.414
Reference velocity, scaled air injection length	-0.144	-0.084	-0.091
Initial particle slip ratio	-0.573	-0.271	-0.115
Initial particle temperature ratio, T_{p0}/T_f	-0.805	-0.174	-0.006

where $\mathcal{P}$ represents any of the parameters investigated. Table 3 provides the exponents n for $\epsilon = 0.05$, 0.5, and 0.95 for five parameters. From Table 3 it can be seen that the particle size effect is relatively independent of extent of reaction with an average exponent of 1.32. The strong influence of initial agglomerate size suggests the need for an extremely well-atomized spray for efficient combustion in a limited-length combustor. The influence of spray drop size distribution on combustor performance is the subject of ongoing research.

Results illustrated in Fig. 3 show that a change in chamber pressure from 1 to 20 atm yields significantly increased burning rates and shortened combustor lengths to achieve $\eta_c = 98\%$. The power-law exponent for burning time dependence on pressure (Table 3) is only a weak function of extent of reaction with an average value of $n = -0.167$. Pressure effects manifest themselves principally through the concentration of reactants at the particle surface and shifts in gas-phase equilibrium.

Figure 4 illustrates the importance of the manner in which air is added into the secondary combustion zone by comparing the effect of the three different secondary-air schedules defined in Table 1. From the figure it can be seen that the earlier the air is introduced, the greater the carbon burnout in a fixed length. This effect is most pronounced at combustion efficiencies less than 98%, e.g., at the 98% level, the required combustor length varies only a few percent among air injection schedules, while at the 90% level, combustor lengths differ 30% between the standard and "spike" air schedule. Two consequences of the early air introduction work together to enhance the agglomerate combustion: first, the production of an oxidizer-rich environment during the early stages of combustion increases reaction rates, and second, the greater slip velocity increases transport rates. For the spike schedule, a minimum gas-phase equivalence ratio of 0.21 is achieved at the termination of air injection ($x/x_a = 1.0$). At this same location, the difference between gas and particle velocity is 23.4 m/s for the spike schedule, while it is only 0.9 m/s for the constant standard air injection schedule. As the agglomerate particles move downstream, both of these effects diminish.

The effect of dimensionless combustor reference velocity, or mass loading, on carbon burnout is shown in Fig. 5. The solid curves represent the cases where only the reference velocity was varied and the air injection length was fixed at $x/x_a = 1.0$. For the dashed lines, the air injection length was scaled with the reference velocity to provide approximate time-similarity so that approximately the same oxidation environment existed at the same time for all three reference velocities. In both cases, an increasing reference velocity requires a greater combustor length for the same combustion efficiency, as one would expect based on residence time considerations alone. Table 3 also shows that burning times decrease with reference velocity, although only a slight dependence is seen for the scaled air injection length. Thus, the major contribution of reference velocity to enhanced combustion in the fixed air length case is the greater availability of oxygen, with enhanced transport playing a relatively minor role.

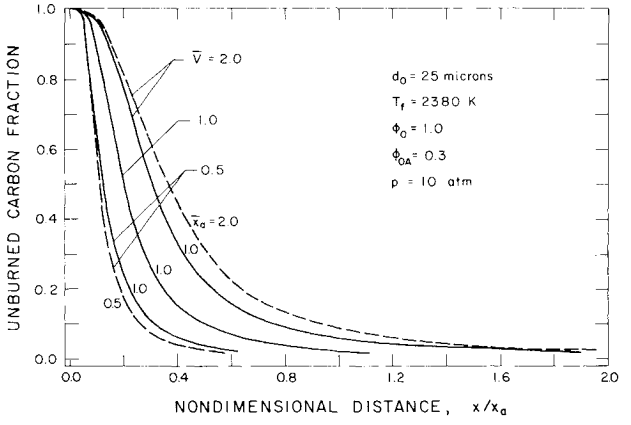

Fig. 5 Unburned carbon fraction vs nondimensional distance for various nondimensional reference velocities.

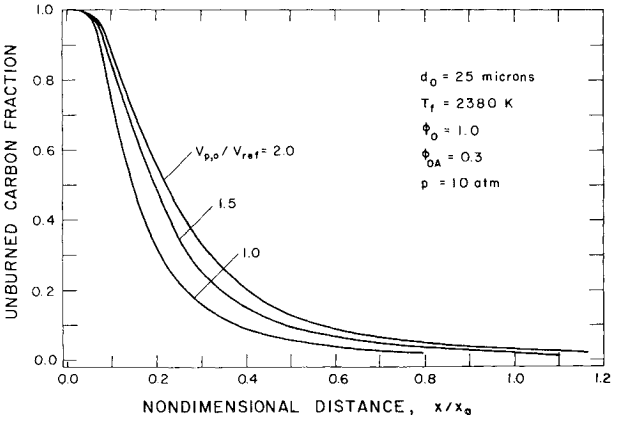

Fig. 6 Unburned carbon fraction vs nondimensional distance for initial particle slip ratios of 1.0, 1.5, and 2.0.

Figure 6 illustrates the effect of initial particle slip velocity on carbon burnout. The principal mechanism causing the less favorable burnout at higher slip ratios is the decreased residence time in a fixed length of the combustor. The time to achieve $\eta_c = 98\%$ was essentially the same for all three initial slip ratios. Table 3 shows the diminishing effect of slip ratio on burnout time as the combustion efficiency or extent of reaction increases. Initial particle preheat had little influence on either burnout length (Fig. 7) or burnout time (Table 3) for combustion efficiencies of practical importance. These results suggest that an improved combustor model should allow for a distribution of initial particle velocities, while particle preheating effects may not have be treated in as much detail.

To achieve desirable rheological properties and stability, various carbon blacks having differing particle sizes, i.e., ultimate particle size, may be used in the formulation of slurry

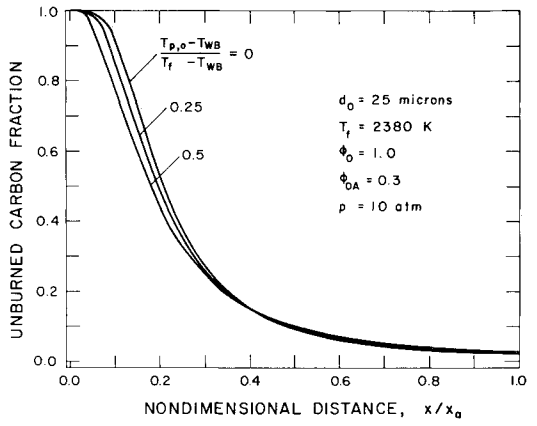

Fig. 7 Unburned carbon fraction vs nondimensional distance for various amounts of agglomerate preheat.

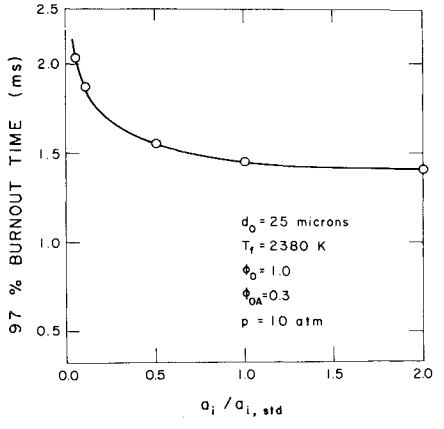

Fig. 8 Effect of area/reactivity factor on the predicted time for 97% carbon burnout.

fuels. Therefore, the effect of the ultimate size of the carbon-black particles composing the agglomerate particles on carbon burnout also was evaluated for ultimate particle sizes of 300 and 70 nm. For all practical purposes, no effect was observed. A similar result was obtained when the influence of catalyst addition to the slurry was simulated by applying the appropriate area/reactivity constants given in Szekely and Faeth.[6] These results strongly suggest that the agglomerate microstructure is relatively unimportant in combustion environments of practical importance where diffusional-controlled combustion dominates the carbon burnout process.

In order to provide additional insight concerning effects of reaction kinetics, the combustor analysis was repeated at the standard conditon while varying the area/reactivity factors over the range of 0.05-2 times the standard values. The results of these calculations are illustrated in Fig. 8, where the 97% burnout time is plotted as a function of the ratio of the adjusted area/reactivity factors to the standard value. As the a_i ratio increases, the burnout time approaches an asymptotic value corresponding to the diffusion-limited case. The results in Fig. 8 indicate that the standard condition is near the diffusion limit, with the near-zero slope representative of a weak influence of kinetics. This finding is consistent with the small effect of carbon-black blend and catalyst noted earlier.

Conclusions

Based on a one-dimensional analysis of a carbon slurry-fueled combustor, several conclusions were obtained. It should be cautioned, however, that most practical combustion systems exhibit three-dimensional characteristics. Therefore, the effects of mixing, local inhomogeneities, particle quenching, and failure to ignite are ignored in the following conclusions.

1) Initial agglomerate diameter, chamber pressure, and secondary-air scheduling all had a significant effect on carbon burnout. The effects of diameter and pressure were essentially independent of the extent of reaction or combustion efficiency, while the effect of early air introduction diminished to near zero as combustion efficiencies approached 100%.

2) Increasing combustor reference velocity greatly increased carbon burnout lengths because of decreased residence times. However, burnout times were significantly decreased by oxygen enrichment associated with increased reference velocities for a fixed air injection length.

3) The effect of particle preheat was relatively insignificant for combustion efficiencies of practical importance; however, variations in initial particle slip velocity produced a substantial effect on predicted combustor performance and should be investigated further.

4) The predicted effects of changing ultimate carbon particle size and addition of catalyst on combustor performance were insignificant, indicating that agglomerate microstructure and reactivity are relatively unimportant in the diffusion-controlled combustion environments typical of practical combustion chamber conditions.

Acknowledgments

This research was sponsored by the Aero Propulsion Laboratory, Wright-Patterson Air Force Base, Contract F33615-82-K-2256, under the technical management of C.R. Martel.

References

[1] Burdette, G. W., Lander, H. R., and McCoy, J. R., "High Energy Density Fuels for Cruise Missiles," AIAA Paper 78-267, 1978.

[2] Salveson, R. H., "Carbon Slurry Fuels for Volume Limited Missiles," AFAPL-TR-79-2122, Nov. 1979.

[3] Bruce, T. W. and Mongia, H., "Compound Cycle Turbofan Engine Task IX: Carbon-Slurry Fuel Combustion Evaluation Program," AFWAL-TR-80-2035, March 1980.

[4] Lavid, M. and Ruth, L. A., "The Combustion of Carbon Slurry Fuel—Experimental Results," *Proceedings of the Fall Technical Meeting—Eastern Section of the Combustion Institute,* The Combustion Institute, Pittsburgh, Pa., Paper 6, Oct. 1980.

[5] Stearns, R. S. and Hall, L. W. Jr., "Carbon Slurry Fuel Formulation and Combustion," AFWAL-TR-82-2105, Oct. 1982.

[6] Szekely, G. A. Jr. and Faeth, G. M., "Combustion Properties of Carbon Slurry Drops," *AIAA Journal*, Vol. 20, 1982, pp. 422-429.

[7] Szekely, G. A. Jr. and Faeth, G. M., "Reaction of Carbon Black Slurry Agglomerates in Combustion Gases," *Nineteenth Symposium (International) on Combustion,* The Combustion Institute, Pittsburgh, Pa., 1982, pp. 1077-1085.

[8] Szekely, G. A. Jr., Turns, S. R., and Faeth, G. M., "Effects of Carbon-Black Properties on Combustion of Carbon-Black Slurry Agglomerates," *Combustion and Flame*, Vol. 58, 1984, pp. 31-43.

[9] Neoh, K. G., Howard, J. B., and Sarofim, A. F., "Soot Oxidation in Flames," *Particulate Carbon Formation During Combustion,* edited by D. C. Seigla and G. W. Smith, Plenum Press, New York, 1981, pp. 261-282.

[10] Libby, P. A. and Blake, T. R., "Theoretical Study of Burning Carbon Particles," *Combustion and Flame,* Vol. 36, Oct. 1979, pp. 139-169.

[11] Libby, P. A. and Blake, T. R., "Burning Carbon Particles in the Presence of Water Vapor," *Combustion and Flame,* Vol. 41, May 1981, pp. 123-147.

[12] Olikara, C. and Borman, G. L., "A Computer Program for Calculating Properties of Equilibrium Combustion Products with Some Applications to I.C. Engines," SAE Paper 750468, 1975.

[13] Lienesch, J. H. and Krieger, R. B., "A Procedure to Compute Composition and Gas Properties of Equilibrium Combustion Products," General Motors Research Laboratories, Warren, Mich., Res. Pub. GMR-3606, March 1981.

[14] Faeth, G. M., "Current Status of Droplet and Liquid Combustion," *Progress in Energy and Combustion Science*, Vol. 3, 1977, pp. 191-224.

[15] White, F. M, *Viscous Fluid Flow,* McGraw-Hill Book Co., New York, 1974.

[16] Turns, S. R., Riddle, S. P., and Faeth, G. M., "Combustion of Agglomerates Formed by Carbon Slurry Fuels," AFWAL-TR-83-2076, Nov. 1983.